



저작자표시-비영리-변경금지 2.0 대한민국

이용자는 아래의 조건을 따르는 경우에 한하여 자유롭게

- 이 저작물을 복제, 배포, 전송, 전시, 공연 및 방송할 수 있습니다.

다음과 같은 조건을 따라야 합니다:



저작자표시. 귀하는 원저작자를 표시하여야 합니다.



비영리. 귀하는 이 저작물을 영리 목적으로 이용할 수 없습니다.



변경금지. 귀하는 이 저작물을 개작, 변형 또는 가공할 수 없습니다.

- 귀하는, 이 저작물의 재이용이나 배포의 경우, 이 저작물에 적용된 이용허락조건을 명확하게 나타내어야 합니다.
- 저작권자로부터 별도의 허가를 받으면 이러한 조건들은 적용되지 않습니다.

저작권법에 따른 이용자의 권리는 위의 내용에 의하여 영향을 받지 않습니다.

이것은 [이용허락규약\(Legal Code\)](#)을 이해하기 쉽게 요약한 것입니다.

[Disclaimer](#)

**Collective Hydrogen Bonding between Amides
Enhances the Basicity of Their Clustered Form in
the Proton Transfer of a Super Photoacid**

Heesu Kim

Department of Chemistry
(School of Molecular Sciences)
Graduate School of UNIST

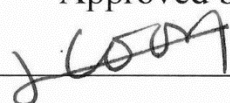
**Collective Hydrogen Bonding between Amides
Enhances the Basicity of Their Clustered Form in
the Proton Transfer of a Super Photoacid**

A thesis
submitted to the Graduate School of UNIST
in partial fulfillment of the
requirements for the degree of
Master of Science

Heesu Kim

12. 10. 2015

Approved by



Advisor

Oh-Hoon Kwon

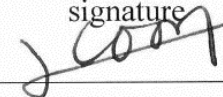
**Collective Hydrogen Bonding between Amides
Enhances the Basicity of Their Clustered Form in
the Proton Transfer of a Super Photoacid**

Heesu Kim

This certifies that the thesis of Heesu Kim is approved.

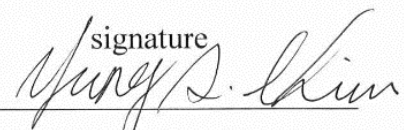
12. 10. 2015

signature



Advisor: Oh-Hoon Kwon

signature



Prof. Yung-Sam Kim

signature



Prof. Bum Suk Zhao

Abstract

The excited state proton transfer (ESPT) of the strong photoacid *N*-methyl-7-hydroxyquinolium (NM7HQ) was studied in the presence of *N*-methylbenzamide (NMB) as a base in the aprotic solvent of acetonitrile. In the ground state, it is found that the complexed form of NM7HQ and NMB exists with a 1:1 ratio with the association constant (K) to $22.2 \pm 1.7 \text{ M}^{-1}$, obtained by using the Benesi-Hilderbrand relation. Also, the cationic photoacid fluorescence lifetime Stern-Volmer relation of fast decay time shows that the ESPT of NM7HQ and NMB has the molecularity of two with amides. Therefore, in the excited state, one more molecule of NMB is needed to the ground state NM7HQ-NMB complex for ESPT. It shows that the hydrogen bonded complex of 2 molecules of NMB can enhance the basicity of the NMB molecule.

Contents

I . Introduction -----	6
II . Methods and Materials -----	7
III. Results -----	8
3.1 Steady-state absorption spectra -----	8
3.2 Steady-state fluorescence spectra -----	8
3.3 Time-resolved fluorescence kinetic profiles -----	9
IV. Discussion -----	10
3.1 Formation of hydrogen bonded complexes at the ground state -----	10
3.2 Chemical kinetics analysis -----	11
3.3 Formation of hydrogen bonded complexes at the excited state -----	12
3.4 Reactivity of monomeric <i>vs</i> clustered bases -----	12
V . Conclusion -----	13
VI. Figures, Schemes and Tables -----	14
VII. Reference -----	22
VIII. Acknowledgements -----	28

List of Figures

Figure 1. Steady-state absorption spectra of 0.1 mM NM7HQ in acetonitrile with addition of NMB. The concentration unit of NMB is given by molar concentration.

Figure 2. Steady-state emission spectra of 0.1 mM NM7HQ in acetonitrile with addition of NMB. Excitation wavelength is 375 nm. The concentration unit of NMB is given by molar concentration.

Figure 3. Fluorescence dynamics of NM7HQ with addition of NMB in acetonitrile. The kinetic profiles of AH^{+*} was excited at 375 nm, and was monitored at 430 nm. The concentration unit of NMB is given by molar concentration. Bi-exponential fits are given by solid lines. The concentration of NMB is given in the panel.

Figure 4. Fluorescence dynamics of NM7HQ with the presence of 0.1069 M NMB in acetonitrile. Excitation wavelength is 375 nm, and monitored wavelengths are 430 nm (lower line, black) and 550 nm (upper line, red). Bi-exponential fits, $I_{\lambda}(t) = A_1e^{-t/\tau_1} + A_2e^{-t/\tau_2}$, are given by solid lines.

Figure 5. Benesi-Hildebrand plot of $[\text{NMB}]^{-1}$ versus reciprocal absorbance in acetonitrile with addition of NMB, indicating a 1:1 stoichiometry. Data were taken at 395 nm. Linear fitted line intercept is the association constant (K).

Figure 6. Stern-Volmer plot for the decrease of the fast decay time monitored at 430 nm versus the concentration of NMB. The molecularity (n) for NMB is ~ 1 . Molecularity was obtained from linear regression fits.

List of Tables

Table 1. Fluorescence time constants obtained from TCSPC measurements depending on the concentration of NMB in acetonitrile.

List of Schemes

Scheme 1. A proposed mechanism of the excited-state proton transfer in this study. The photoacid is NM7HQ, and the base is NMB. NM7HQ-NMB 1:1 complex is in the ground state when NMB was added, due to the high binding constant (K).

Explanation of abbreviations

ESPT	- Excited state proton transfer
NM7HQ	- <i>N</i> -methyl-7-hydroxyquinolinium
NMB	- <i>N</i> -methylbenzamide
AH⁺	- Cation form of photoacid
AH⁺*	- Excited state of cation form of photoacid
A	- Keto form of photoacid
A*	- Excited state of keto form of photoacid

Introduction

Nature of the amide group has long been of fundamental interest, due to its role as a repeating unit in biological and industrial polymers. Especially, amide-water and amide-amide hydrogen bonding interactions affect the secondary and tertiary structure, protein folding, receptor-ligand complex and dynamics of polymers¹⁻⁴.

Furthermore, amide functionality is very common in life, as proteins play a crucial role in chemical and biological processes such as, storage and transportation of molecules (hemoglobin), mechanical support (collagen), immune protection (antibody) and catalytic enzyme⁵. For protein folding, many amide groups exchange hydrogen bonds with other chain amides. This amide-amide internal hydrogen bond has an ability to affect the folded structure of proteins. The folded structures in the proteins are strongly dependent upon the properties of the medium³.

The amides and *N*-methyl amides have the ability to strongly associate with molecules. They are both stronger hydrogen-bond donors and acceptors than water⁶. The main competitors for the amide's proton donor (N-H) site in a biological environment are nearby side chain C=O linkages and the oxygen of nearby water molecules. The amide N-H and the water O-H compete for the carbonyl acceptor sites on the amide².

Also, theoretical calculations suggest that enzymatic catalysis is determined by charge rearrangement in the transition state of hydrogen bond⁷, and a large difference of dipole moments of the amide group and the hydroxyl group affects a stronger forming of hydrogen bonding between amide group-hydroxyl groups⁸. The amide group is an electron withdrawing group, so the existence of another amide will enhance the electrophilicity of amide by an inductive effect. When the two amides are closer, the inductive effect will be larger and the quenching rate will be higher⁹.

The hydrogen bonding is also influenced by Kamlet-Taft parameters, α and β . The α scale of the hydrogen bond donor acidity means the ability to donate proton hydrogen bond. The β scale of hydrogen bond acceptor basicity describes the ability to accept proton hydrogen bond¹⁰. Chirality affects hydrogen bonding, where homochiral molecules have a stronger hydrogen bond than that of

racemic molecules¹¹.

Proton transfer has been attracting many research groups because it performs a key role in a wide variety of chemicals and biological sciences¹²⁻¹⁷. In biology, proton transfer is key for enzymatic hydrolysis, proton pumps in membrane proteins, the photomutagenesis of DNA, and the fluorescence of green fluorescent proteins¹⁸⁻²⁶. Water autoionization, fast diffusion of hydronium and hydroxide ions, and acid-base reactions are the result of proton transfer in chemistry²⁷⁻³⁰.

To investigate the process of reactions unveiling the hidden reaction intermediates or mechanisms, real-time tracking is crucial³¹. In this case, absorbance and fluorescence spectroscopy are useful for emissive reactants and products in photoinduced reactions. In this regards, time dependent populations of reactants and products is reflected by time-resolved fluorescence kinetic profiles. Excited-state proton transfer (ESPT) of photoacids has been researched by using the time-resolved fluorescence spectroscopy³²⁻⁴⁴.

The 7-hydroxyquinoline has a more extreme behavior, because the hydroxyl groups undergo a reduction in pK_a of approximately from 9 to 11 units in aqueous solution. In this case, proton transfer rates are much faster. The photoinduced tautomerization of 7-hydroxyquinoline and its derivatives like *N*-methyl-7-hydroxyquinolinium (NM7HQ) has been researched by several groups like the solvent bridge proton relay mechanism in solutions for solvent mediated pathway for phototautomerization⁴⁵.

In this study, we used *N*-methylbenzamide (NMB) for, acetonitrile, and NM7HQ quencher, solvent, and photoacid respectively. And we studied the ground state of interaction between NM7HQ and NMB, so we can track the effect of ground state amide-photoacid complex and the effect of enhanced basicity of complexed amides in the ESPT through the collective hydrogen bonding between amides. With this study, we can model ESPT of protein and their proton transfer mechanism, such as enzyme catalytic reactions.

Methods and materials

N-methylbenzamide (99%) from Alfa Aesar, 7HQ (99%) from Acros, Acetonitrile (anhydrous) from Sigma-Aldrich, iodomethane (99%) from Sigma-Aldrich and NM7HQ was synthesized. NM7HQ was synthesized by refluxing 7-hydroxyquinoline (>99%) from Sigma-Aldrich with methyl iodide (>99%) from Sigma-Aldrich in toluene for 2 days. The solid was precipitated by adding diethyl ether to the solution, separated, and recrystallized⁴⁵. The samples were prepared by mixing the acetonitrile solution with NMB for binary mixtures with $[NM7HQ] = 1 \times 10^{-4}$ M. Acetonitrile was kept over 4 Å molecular sieves, and NMB was used as received in solid.

UV-vis absorption spectra was obtained using a UV-Vis spectrophotometer (V-730, Jasco) and Photoluminescence spectra was measured with a fluorometer instrument (QM-400, Photon Technology International). Picosecond-resolved fluorescence decay profiles were measured using a time-correlated single photon count spectrometer (Fluotime 300, PicoQuant) with a picosecond laser diode emitting 375 nm (LDH-D-C-375, PicoQuant). The total instrument response function (IRF) was ~150 ps. The fluorescence decay profiles deconvolution was performed by using a fitting software (PicoQuant, Fluofit). All measurements were performed at room temperature.

Results

1. Steady-state absorption spectra

Figure 1 presents that the Absorption spectra of NM7HQ in acetonitrile with addition of NMB. In neat acetonitrile, the main absorption band of NM7HQ is 355 nm, and another band around 450 nm. These 355 nm and 450 nm bands are the result of lowest electronic absorption of cationic (AH^{+*}) and its conjugate base (**A**). When NMB was added, the 450 nm band grew slowly and the 355 nm band showed a gradually decreasing peak.

There is also a red-shift in the 355 nm spectra upon gradual addition of NMB. It means that the complex between NM7HQ and NMB makes a lower energy state due to production of hydrogen bonding. Also, the increasing of 450 nm band shows that the increase of deprotonated form of AH^+ (**A**) species, and decreasing of 355 nm band shows that the decrease of AH^{+*} species. It is because proton transfer can occur by addition of NMB molecule.

2. Steady-State fluorescence spectra

Figure 2 shows the emission spectra of NM7HQ in acetonitrile with addition of NMB, with excitation at 375 nm. 430 nm single fluorescence band was observed in acetonitrile because of exclusive existence of AH^+ species. Absorption spectra showed that the 355 nm band of AH^+ , 430 nm emission band originated from excited photoacid (AH^+).

By adding NMB, a new band increases around 520nm and gradually decreases 430 nm band. When excited at 450 nm, deprotonated form of AH^+ (A) absorbs light in ground state. Therefore 520 nm emission band can be assigned to A excited state species (A^*). There is a band shift of 430 nm emission band, due to the increase of 520 nm band.

3. Time-resolved fluorescence kinetic profiles

Fluorescence kinetic profiles were measured to observe the population changes of AH^{+*} and the A^* species. Kinetic profiles were monitored at 430 nm to probe AH^{+*} . And A^* was collected at 550 nm to minimize the spectral overlapping and interference by the red tail of AH^{+*} fluorescence.

Figure 3 shows the fluorescence kinetic profiles of AH^{+*} in acetonitrile with the addition of NMB. Table 1 shows that the kinetic constants have a bi-exponential fit. In range of 0 M to 0.1069 M of NMB, the AH^{+*} fluorescence was found to decay bi-exponentially. Two AH^{+*} decay time constants decrease gradually with increasing concentration of NMB. Decay time constants are changed from 9.13 ns to 8.24 ns (free NM7HQ component), and the other one changed from 3.5 ns to 2.03 ns (NM7HQ – NMB complexed component). The fluorescence kinetic profiles of A^* is in table 1. The bi-exponential fit showed a rise component ~ 7.24 ns lifetime up to $[\text{NMB}] = 0.0218$ M. and the decay component changed from 8.62 ns to 8.3 ns.

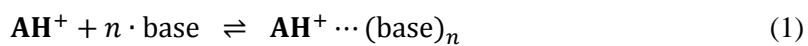
Shown as table 1, decay time of free NM7HQ component changed from 9.13 ns to 8.24 ns at 445 nm. Also, decay time changed from 8.62 ns to 8.30ns at 580nm. The decay time of free NM7HQ was changed slowly. The fractional decay time values were gradually decreased from 93.4 % to 40.0 %.

Decay time of NM7HQ-NMB complexed component was decreased from 3.50 ns to 2.03 ns at 445 nm. And rise time was obtained from 7.24 ns to 1.57 ns. The decay time fractional amplitude was increased from 6.6 % to 60.0 % at 445 nm, however fractional amplitude of rise time was decreased from -70.0 % to -10.6 %.

Discussion

1. Formation of Hydrogen bonded complexes at the ground state

Fluorescence decay of \mathbf{AH}^{+*} can be originated from two components, as shown in figures 4, 5 and table 1. First, both \mathbf{AH}^{+*} and \mathbf{A}^* fluorescence showed bi-exponential decay. Also, there are only two global lifetimes at $[\text{NMB}] = 0.1069 \text{ M}$ time-resolved emission spectra. In this case, inside of the binary mixture solution, there may be two components. The first one is free NM7HQ, and the other one is NM7HQ – NMB complex. The Acetonitrile-NM7HQ Solution after NMB was added, NMB may associate with free NM7HQ in ground state. This equilibrium can be described by equation 1.



From equation 1, NMB can act as a base in this equilibrium. Also, the formation of \mathbf{A} is not considered in this ground state equilibrium. An expression for the Benesi-Hilderbrand^{46,47} plot has a relation of the molar concentration of base (C) to the observed absorbance (A). Then, the association constant (K) of $\mathbf{AH}^+ \cdots (\text{base})_n$ can be expressed by equation 2.

$$\frac{1}{C^n} = Ka(\varepsilon_2 - \varepsilon_1) \frac{1}{A - A_0} - K \quad (2)$$

A denotes the absorbance of measured at certain concentration, and the absorbance measured in neat acetonitrile is A_0 . a is the initial concentration of NM7HQ, and molar extinction coefficient of \mathbf{AH}^+ and $\mathbf{AH}^+ \cdots (\text{base})_n$ is ε_1 and ε_2 . The linear relationship between $1/C$ and $1/(A - A_0)$ in figure 5 indicates that \mathbf{AH}^+ and NMB molecules form 1:1 complex with K of $22.2 \pm 1.7 \text{ M}^{-1}$ in ground state. Therefore, there are NM7HQ-NMB complexed component in ground state, and the complexed form of NM7HQ and NMB is the dominant form in ground state.

2. Chemical kinetics analysis

Due to the existence of 1:1 NM7HQ-NMB complex in the ground state, there are two hydrogen bonded configurations for the photoacid: free \mathbf{AH}^{+*} and $\mathbf{AH}^{+*}\cdots\text{NMB}$. These two species are possible to undergo ESPT with different molecularity of added NMB. \mathbf{AH}^{+*} fluorescence monitored at 430 nm showed bi-exponential decays (Table 1). Furthermore, the association constant (K) is $22.2 \pm 1.7 \text{ M}^{-1}$, is the dominant component after adding NMB in acetonitrile–NM7HQ solution.

In Scheme 1, k_{diff} is the rate constant of the diffusion of NMB to associate with another NMB. k_{pt} is the rate constant for proton transfer of $\mathbf{AH}^{+*}\cdots(\text{NMB})_2$ component. If k_{diff} is much smaller than k_{pt} , then a pseudo two-state model, in which the overall rate is determined by the diffusional formation of a reactive hydrogen bonded complex. Time-resolved kinetic profiles $[\text{NMB}] \leq 0.1069\text{M}$ are a diffusion-controlled region. We can derive equations 3 and 4 for pseudo two-state model to show the time dependence of $[\mathbf{AH}^{+*}]$ and $[\mathbf{A}^*]$.

$$[\mathbf{AH}^{+*}] = [\mathbf{AH}^{+*}]_0 e^{-(k_{\text{AH}^{+*}} + k_{\text{pt}})t} \quad (3)$$

$$[\mathbf{A}^*] = \left(\frac{[\mathbf{AH}^{+*}]_0 \cdot k_{\text{pt}}}{k_{\text{AH}^{+*}} + k_{\text{pt}} - k_{\mathbf{A}^*}} \right) [e^{-k_{\mathbf{A}^*}t} - e^{-(k_{\text{AH}^{+*}} + k_{\text{pt}})t}] \quad (4)$$

k_{pt} is the overall diffusion-controlled rate constant of ESPT, and $k_{\text{AH}^{+*}}$ and $k_{\mathbf{A}^*}$ are the rate constants for the relaxation of \mathbf{AH}^{+*} and \mathbf{A}^* . In typical ESPT, $(k_{\text{AH}^{+*}} + k_{\text{pt}})$ is usually larger than $k_{\mathbf{A}^*}$ in equation 4, so the decay time of a parent photoacid matches well with the rise time of a conjugate base. It is the same as in this study.

Table 1 shows that the decay time of \mathbf{AH}^{+*} fluorescence monitored at 430 nm and the decay time of \mathbf{A}^* fluorescence monitored at 550 nm are almost the same and become gradually shorter with the addition of NMB. With equation 4, in this ESPT mechanism, $(k_{\text{AH}^{+*}} + k_{\text{pt}})$ is larger than $k_{\mathbf{A}^*}$. This explains that the decay time at 550 nm is related to $k_{\mathbf{A}^*}$. Also, the rise time of $k_{\mathbf{A}^*}$ is related to $(k_{\text{AH}^{+*}} + k_{\text{pt}})$, because it is related to concentration of NMB.

3. Formation of hydrogen bonded complexes at the excited state

To find the stoichiometric number (n) of the NMB participating in the deprotonation of the photoacid (molarity), we related the obtained k_{pt} from τ , $\tau = (k_{AH^{++}} + k_{pt})^{-1}$, to a simple n -th order empirical expression^{48,49} on quenching of photoacid as:

$$k_{pt} = k_0[\text{base}]^n \quad (5)$$

k_0 is the unimolecular rate constant for the deprotonation. Accordingly, we have examined the quenching rate of AH^{++} applying the n -th order expression to the dynamic Stern-Volmer relation:

$$\frac{\Delta\tau}{\tau} = k_0\tau_0[\text{base}]^n \quad (6)$$

Where $\Delta\tau = \tau_0 - \tau$, τ_0 is the lifetime of photoacid without base. Base is a quencher of the AH^{++} fluorescence by accepting a proton to change AH^{++} to A^+ . Figure 6 indicates that one (1.13 ± 0.07) NMB molecule is required for NM7HQ-NMB complexed component. However there are no proton transfers of free NM7HQ, because there is no existence of another rise component, which means there is no pathway like the proton transfer of NM7HQ directly with two molecules of NMB.

4. Reactivity of monomeric vs clustered bases

We showed that the non-aqueous acid-base reaction can be facilitated by association of the complexed $AH^{++} \cdots NMB$ and one more NMB molecule. The two complexed NMB molecules have enhanced basicity compared to one molecule of NMB. The reported solvation parameter of NMB is $\alpha_2^H = 0.35$, and $\beta_2^H = 0.73$ (α_2^H and β_2^H are the solute's effective hydrogen-bond acidity and hydrogen-bond basicity parameters)⁵⁰. Similarly, Kamlet-Taft parameters of ethanol is $\alpha = 0.83$ and $\beta = 0.77$. In ethanol, two molecules of alcohol can do proton transfers directly with AH^{++} because of the existence of free AH^+ in ground state dominantly. Therefore, two molecules are needed overall of NMB for proton transfer in this mechanism. Collaboration of two NMB molecules enhances the

basicity, of which the hydrogen bond cluster is an effective Brønsted base⁵¹.

In this study, the majority of \mathbf{AH}^+ molecules exist as complexed form in the ground state. Upon excitation undergo the diffusion-controlled proton transfer, which is reflected by the fast decay component, whose lifetime shortens with the concentration of NMB. In this mechanism, the complexed form makes hydrogen bond between the enol group of \mathbf{AH}^+ and NMB molecule, but the complexed form does not perform a proton transfer. Then, another NMB molecule approaches the complexed one to form a linearly configured amide dimer. In this case, the second NMB molecule accepts the hydrogen bond from the complexed one. This mechanism enhances the basicity of the first NMB molecule already bounded with \mathbf{AH}^{+*} .

Conclusion

Photoacid NM7HQ forms a hydrogen bond complex with two NMB molecules for ESPT. The photoacid is also found to form dominantly as a 1:1 ratio hydrogen bond complex in aprotic medium, and NM7HQ-NMB complex in the ground state. Therefore, the ground state complexed NM7HQ-NMB component needed one more NMB molecule in excited state for ESPT. It shows that the hydrogen bonded complex of 2 molecules of NMB can enhance the basicity of NMB molecules.

Figures, Schemes and Tables

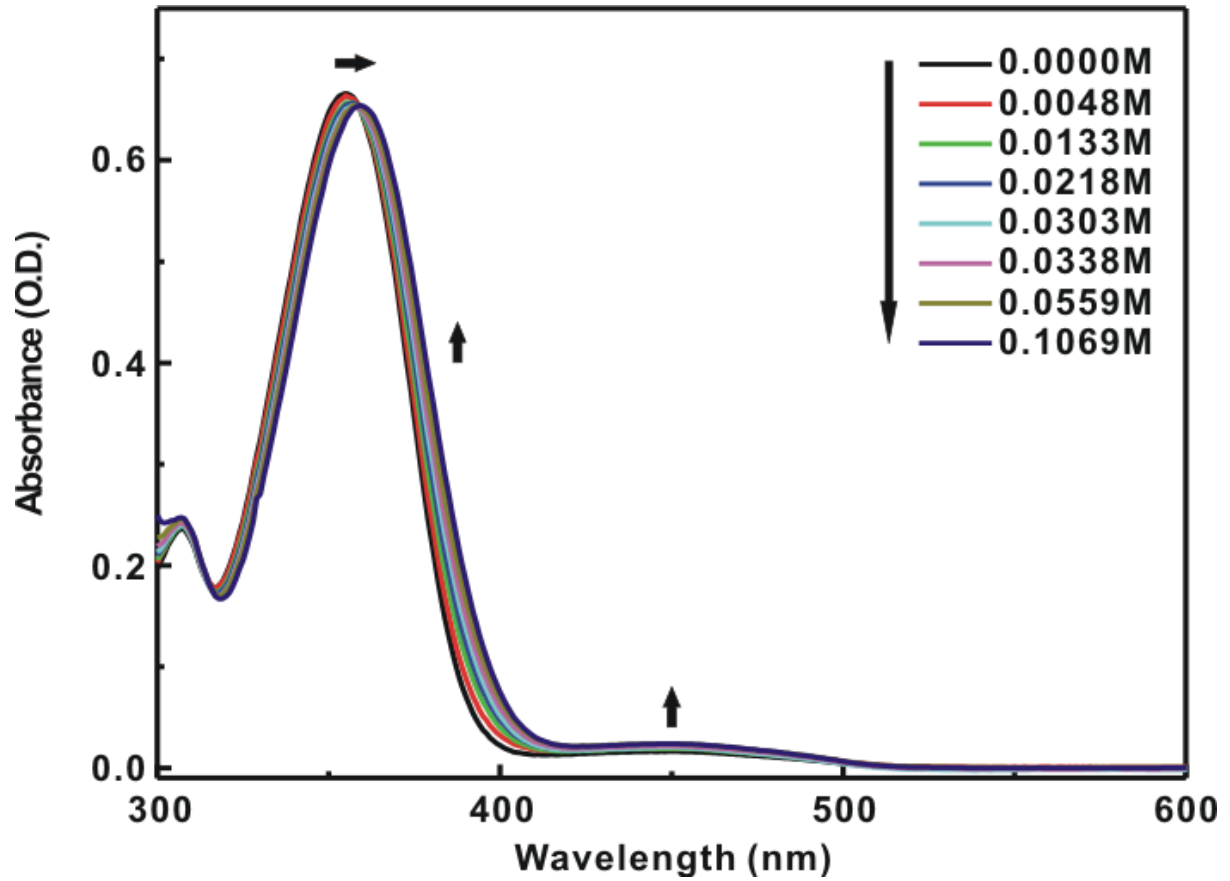


Figure 1. Steady-state absorption spectra of 0.1mM NM7HQ in acetonitrile with addition of NMB. The concentration unit of NMB is given by molar concentration.

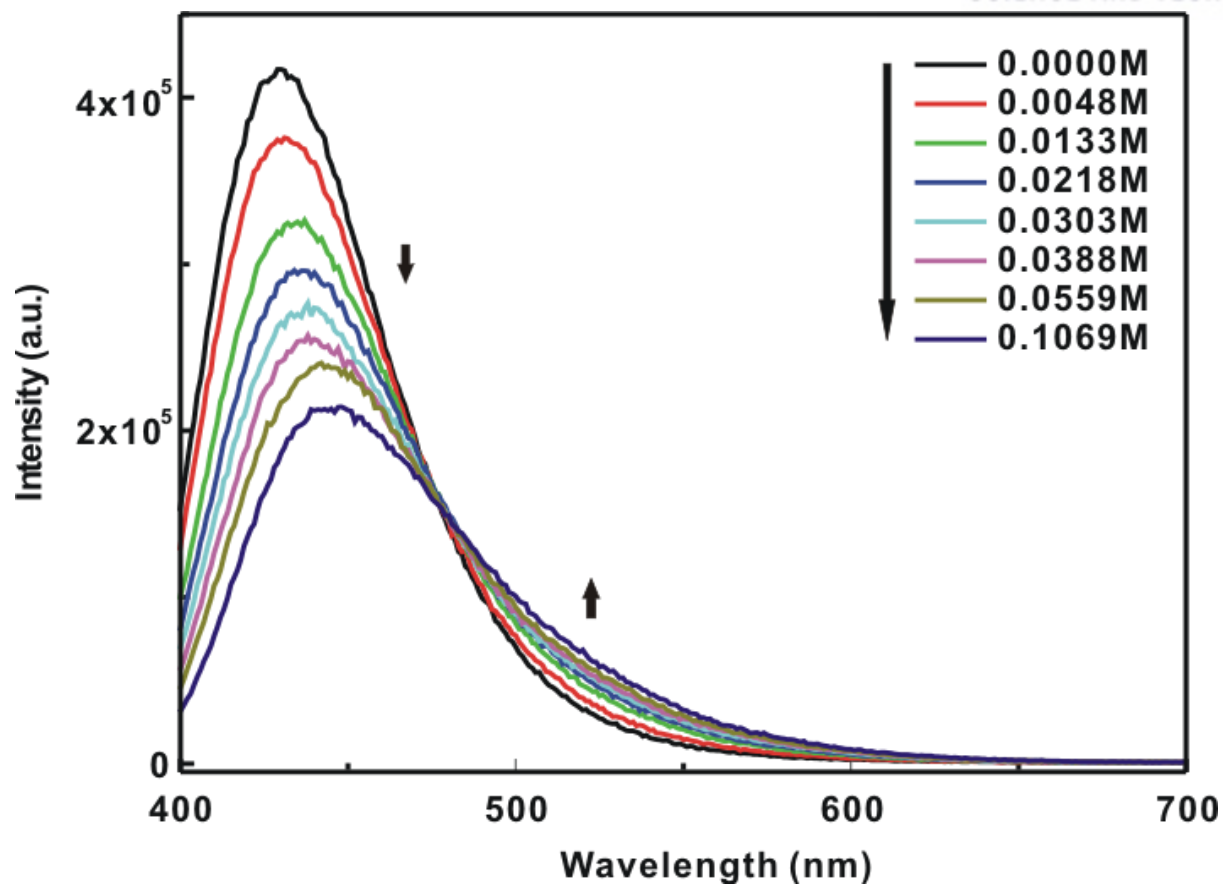


Figure 2. Steady-state emission spectra of 0.1 mM NM7HQ in acetonitrile with addition of NMB. Excitation wavelength is 375 nm. The concentration unit of NMB is given by molar concentration.

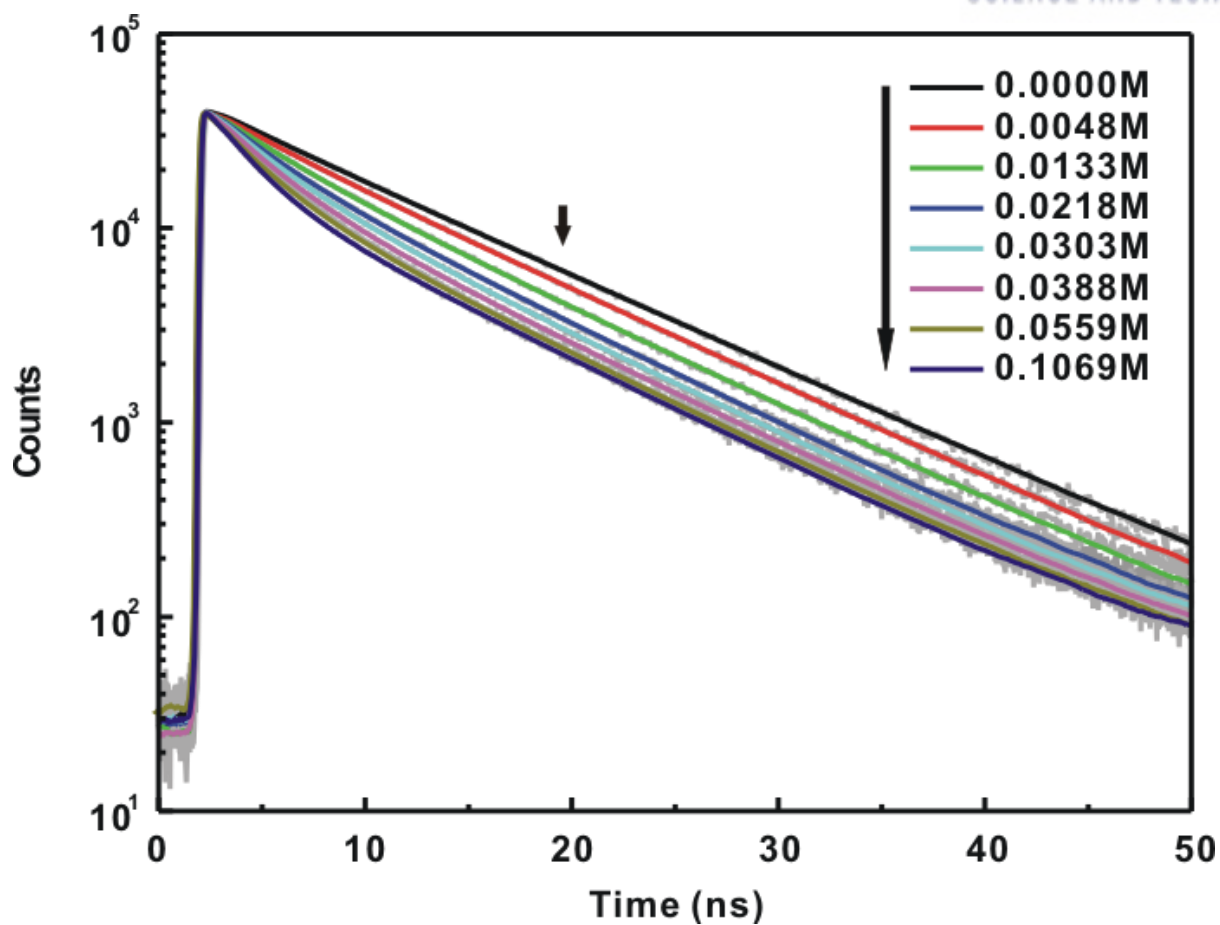


Figure 3. Fluorescence dynamics of NM7HQ with addition of NMB in acetonitrile. The kinetic profiles of AH^{+*} was excited at 375 nm, and was monitored at 430 nm. The concentration unit of NMB is given by molar concentration. Bi-exponential fits are given by solid lines. The concentration of NMB is given in the panel.

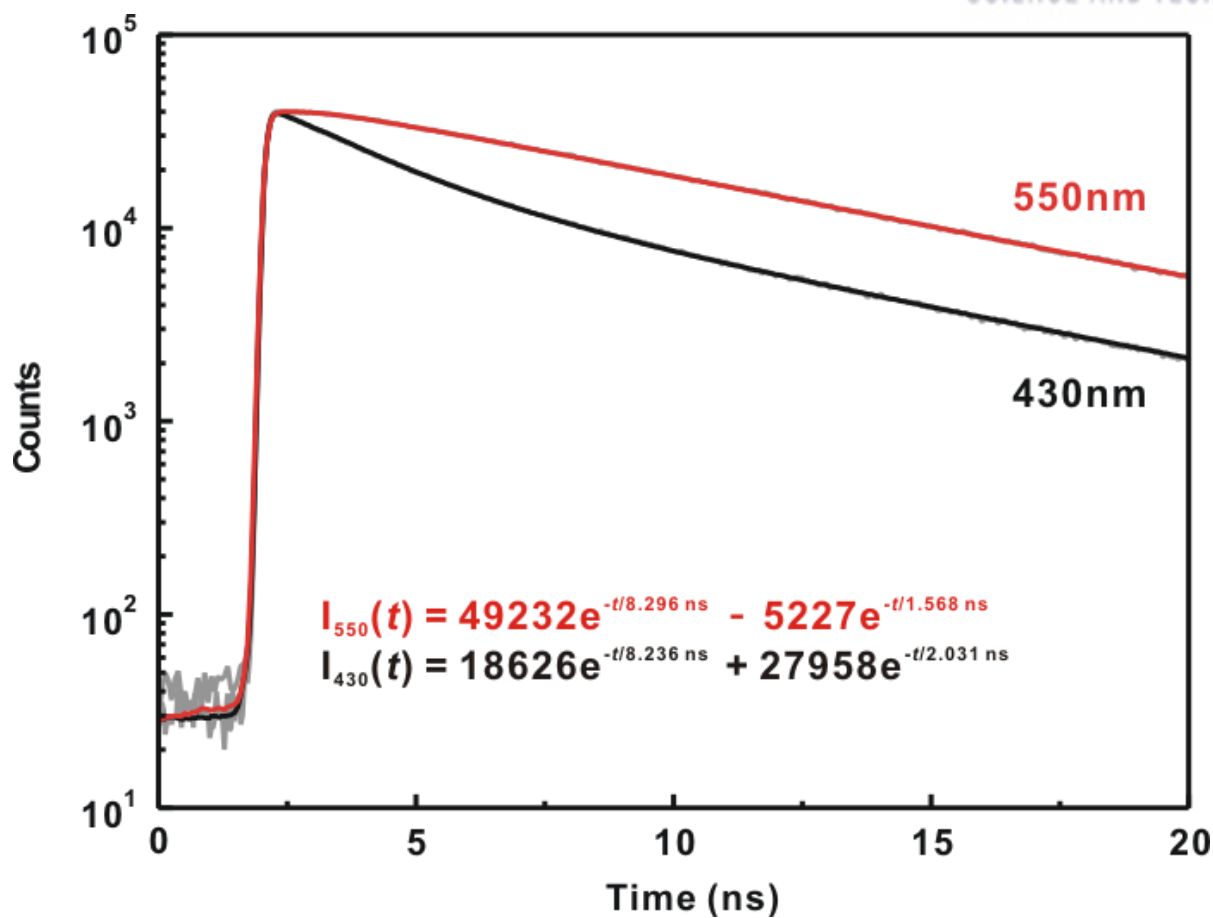


Figure 4. Fluorescence dynamics of NM7HQ with the presence of 0.1069 M NMB in acetonitrile. Excitation wavelength is 375 nm, and monitored wavelengths are 430 nm (lower line, black) and 550 nm (upper line, red). Bi-exponential fits, $I_{\lambda}(t) = A_1e^{-t/\tau_1} + A_2e^{-t/\tau_2}$, are given by solid lines.

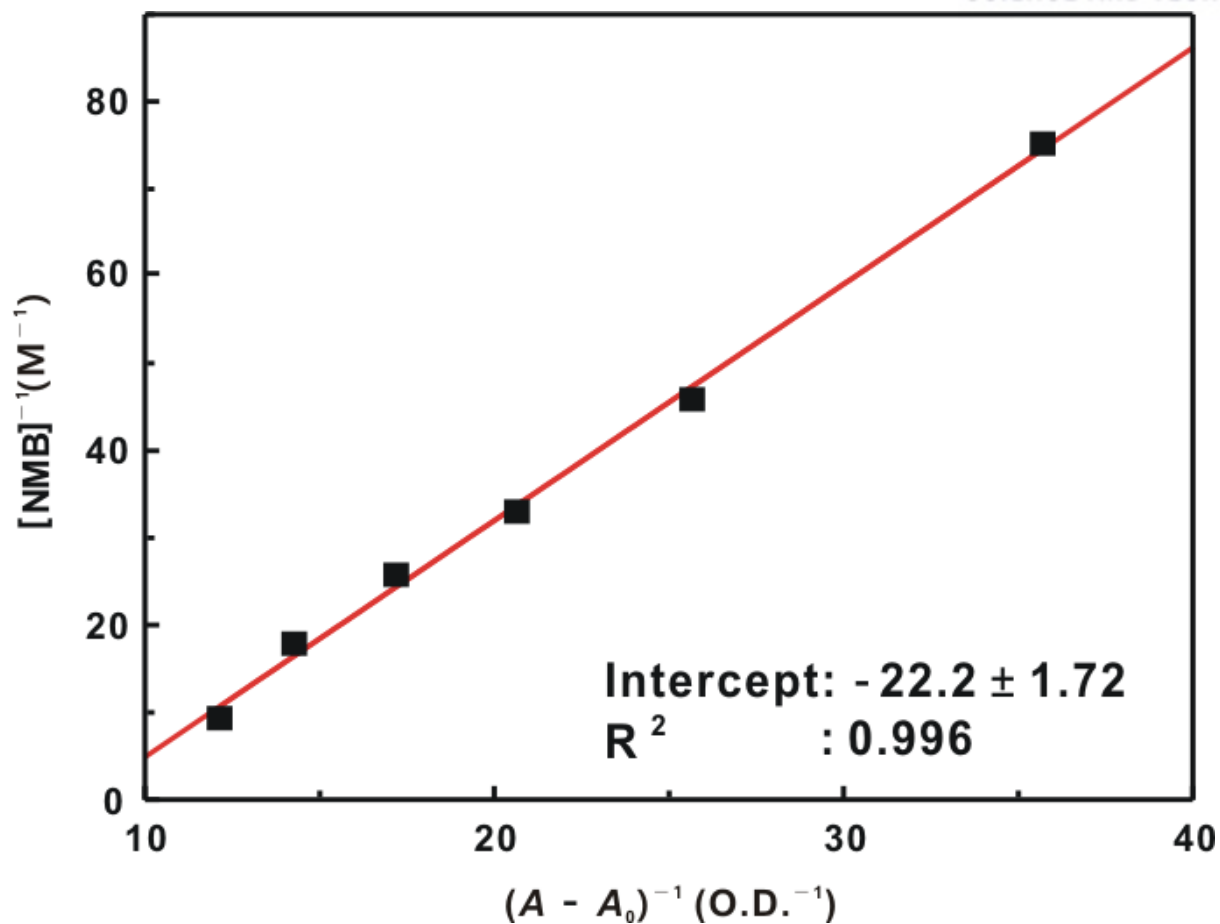


Figure 5. Benesi-Hildebrand plot of $[NMB]^{-1}$ versus reciprocal absorbance in acetonitrile with addition of NMB, indicating a 1:1 stoichiometry. Data were taken at 395 nm. Linear fitted line intercept is the association constant (K).

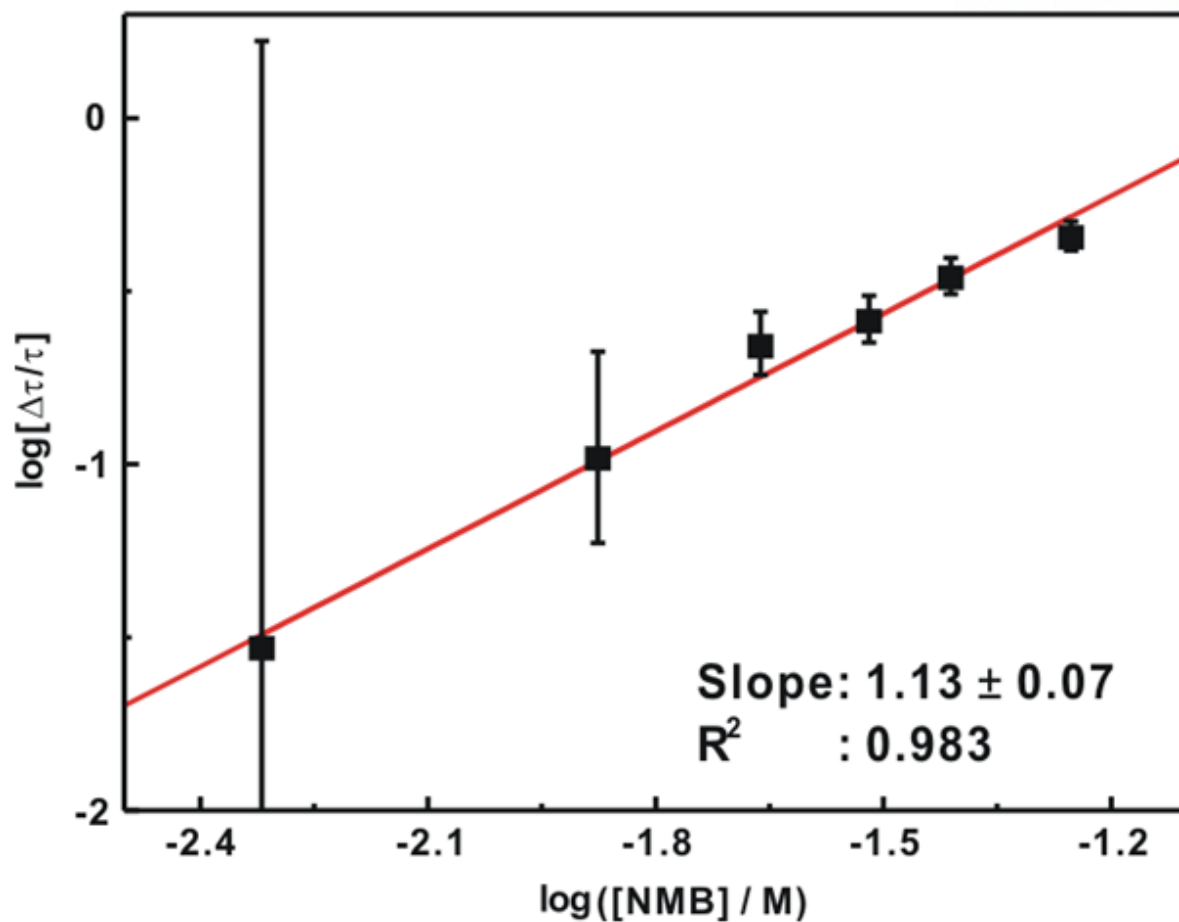
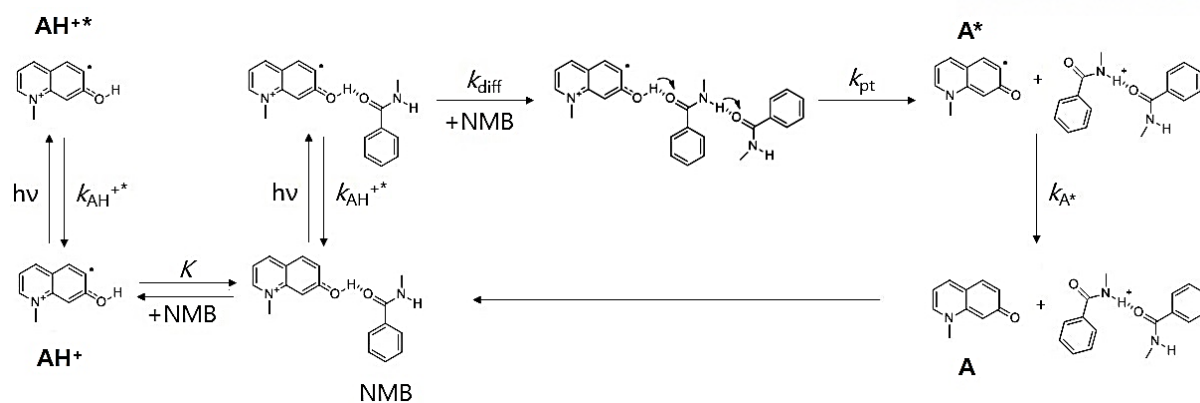


Figure 6. Stern-Volmer plot for the decrease of the fast decay time monitored at 430 nm versus the concentration of NMB. The molecularity (n) for NMB is ~ 1 . Molecularity was obtained from linear regression fits.

Table 1. Fluorescence time constants obtained from TCSPC measurements depending on the concentration of NMB in acetonitrile.

[NMB] (M)	$\lambda_{\text{mon}}^{\text{a}}$ (nm)	Decay time (ns)		Rise time (ns)	χ^2
0.0000	445	9.13 (93.4%) ^b	3.50 (6.6%)		1.062
	580	8.62 (70.9%)	0.99 (29.1%)		1.861
0.0048	445	8.88 (84.0%)	3.40 (16.0%)		1.241
	580	9.35 (73.9%)	0.86 (26.1%)		1.220
0.0133	445	8.61 (70.4%)	3.17 (29.6%)		1.364
	580	9.62 (80.7%)	0.38 (19.3%)		1.975
0.0218	445	8.37 (53.5%)	2.85 (39.5%)		1.172
	580	8.09 (100%)		7.24 (-70.0%) ^c	1.247
0.0303	445	8.37 (53.5%)	2.78 (46.5%)		1.201
	580	8.03 (100%)		6.85 (-60.3%)	1.489
0.0388	445	8.32 (48.4%)	2.60 (51.6%)		1.193
	580	8.39 (100%)		5.35 (-26.6%)	1.329
0.0559	445	8.33 (43.4%)	2.41 (56.6%)		1.227
	580	8.43 (100%)		3.82 (-16.6%)	1.199
0.1069	445	8.24 (40.0%)	2.03 (60.0%)		1.163
	580	8.30 (100%)		1.57 (-10.6%)	1.073

^aMonitored wavelength of fluorescence. ^bDecay time values of initial fractional amplitudes percentage of each component. ^cRise time values of initial fractional amplitudes percentage of each component.



Scheme 1. A proposed mechanism of the excited-state proton transfer in this study. The photoacid is NM7HQ, and the base is NMB. NM7HQ-NMB 1:1 complex is in the ground state when NMB was added, due to the high binding constant (K).

References

- (1) Dixon, D. A.; Dobbs, K. D. Amide-Water and Amide-Amide Hydrogen Bond Strength. *J. Phys. Chem.* **1994**, *98*, 13435–13439.
- (2) Johansson, A.; Kollman, P.; Rothenberg, S.; McKelvey, J. Hydrogen Bonding Ability of the Amide Group. *J. Am. Chem. Soc.* **1974**, *96*, 3794–3800.
- (3) Eberhardt, E. S.; Raines, R. T. Amide-Amide and Amide-Water Hydrogen Bonds: Implications for Protein Folding and Stability. *J. Am. Chem. Soc.* **1994**, *116*, 2149–2150.
- (4) Hubbard, R. E.; Kamran Haider, M. Hydrogen Bonds in Proteins: Role and Strength. In *Encyclopedia of Life Sciences*; John Wiley & Sons, Ltd: Chichester, UK, 2010; Vol. 1, pp. 1–6.
- (5) Montalbetti, C. A. G. N.; Falque, V. Amide Bond Formation and Peptide Coupling. *Tetrahedron* **2005**, *61*, 10827–10852.
- (6) Chang, Y. J.; Castner, E. W. Femtosecond Dynamics of Hydrogen-Bonding Solvents. Formamide and N-Methylformamide in Acetonitrile, DMF, and Water. *J. Chem. Phys.* **1993**, *99*, 113.
- (7) Shan, S.; Herschlag, D. Energetic Effects of Multiple Hydrogen Bonds. Implications for Enzymatic Catalysis. *J. Am. Chem. Soc.* **1996**, *118*, 5515–5518.
- (8) J Brydson. *Plastics Materials*; 6th ed.; Butterworth-Heinemann: Oxford, 1995.
- (9) Chen, Y.; Liu, B.; Yu, H. T.; Barkley, M. D. The Peptide Bond Quenches Indole Fluorescence. *J. Am. Chem. Soc.* **1996**, *118*, 9271–9278.
- (10) Kamlet, M. J.; Abboud, J.-L. M.; Abraham, M. H.; Taft, R. W. Linear Solvation Energy

- Relationships. 23. A Comprehensive Collection of the Solvatochromic Parameters,. *J. Org. Chem.* **1983**, *48*, 2877–2887.
- (11) Solntsev, K. M.; Tolbert, L. M.; Cohen, B.; Huppert, D.; Hayashi, Y.; Feldman, Y. Excited-State Proton Transfer in Chiral Environments. 1. Chiral Solvents. *J. Am. Chem. Soc.* **2002**, *124*, 9046–9047.
- (12) Eigen, M. Proton Transfer, Acid-Base Catalysis, and Enzymatic Hydrolysis. Part I: Elementary Processes. *Angew. Chem. Int. Ed.* **1964**, *3*, 1–19.
- (13) Bountis, T. *Proton Trasfer in Hydrogen-Bonded Systems*; Springer Science & Business Media: New York, 2012.
- (14) Maréchal, Y. *The Hydrogen Bond and the Water Molecule*; Elsevier: Amsterdam, 2007.
- (15) Bell, R. P. *The Proton in Chemistry*; Springer US: Boston, MA, 1973.
- (16) *Hydrogen-Transfer Reactions*; Hynes, J. T.; Klinman, J. P.; Limbach, H.-H.; Schowen, R. L., Eds.; Wiley-VCH Verlag GmbH & Co. KGaA: Weinheim, Germany, 2006.
- (17) Gutman, M.; Nachliel, E. Time-Resolved Dynamics of Proton Transfer in Proteinous Systems. *Annu. Rev. Phys. Chem.* **1997**, *48*, 329–356.
- (18) Agre, P. Aquaporin Water Channels (Nobel Lecture). *Angew. Chem. Int. Ed.* **2004**, *43*, 4278–4290.
- (19) Å delroth, P. Special Issue on Proton Transfer in Biological Systems. *Biochim. Biophys. Acta* **2006**, *1757*, 867–870.
- (20) Cossio, M. L. T.; Giesen, L. F.; Araya, G.; Pérez-Cotapos, M. L. S.; Vergara, R. L.; Manca, M.; Tohme, R. A.; Holmberg, S. D.; Bressmann, T.; Lirio, D. R.; *et al.* *Dynamics in Enzyme*

- Catalysis*; Klinman, J.; Hammes-Schiffer, S., Eds.; Topics in Current Chemistry; Springer Berlin Heidelberg: Berlin, Heidelberg, 2013.
- (21) Li, J.; Liu, Z.; Tan, C.; Guo, X.; Wang, L.; Sancar, A.; Zhong, D. Dynamics and Mechanism of Repair of Ultraviolet-Induced (6-4) Photoproduct by Photolyase. *Nature* **2010**, *466*, 887–890.
- (22) Löwdin, P.-O. Quantum Genetics and the Aperiodic Solid. *Adv. Quantum Chem.* **1966**, *2*, 213–360.
- (23) Kwon, O.-H.; Zewail, A. H. Double Proton Transfer Dynamics of Model DNA Base Pairs in the Condensed Phase. *Proc. Natl. Acad. Sci. U. S. A.* **2007**, *104*, 8703–8708.
- (24) Zhang, Y.; de La Harpe, K.; Beckstead, A. A.; Improta, R.; Kohler, B. UV-Induced Proton Transfer between DNA Strands. *J. Am. Chem. Soc.* **2015**, *137*, 7059–7062.
- (25) Tsien, R. Y. The Green Fluorescent Protein. *Annu. Rev. Biochem.* **1998**, *67*, 509–544.
- (26) Fang, C.; Frontiera, R. R.; Tran, R.; Mathies, R. A. Mapping GFP Structure Evolution during Proton Transfer with Femtosecond Raman Spectroscopy. *Nature* **2009**, *462*, 200–204.
- (27) Codorniu-Hernández, E.; Kusalik, P. G. Probing the Mechanisms of Proton Transfer in Liquid Water: Fig. 1. *Proc. Natl. Acad. Sci. U. S. A.* **2013**, *110*, 13697–13698.
- (28) Lee, S. H.; Rasaiah, J. C. Proton Transfer and the Diffusion of H⁺ and OH⁻ Ions along Water Wires. *J. Chem. Phys.* **2013**, *139*, 124507.
- (29) Gutman, M.; Nachliel, E. The Dynamic Aspects of Proton Transfer Processes. *Biochim. Biophys. Acta. Bioenerg.* **1990**, *1015*, 391–414.
- (30) Voth, G. A. Computer Simulation of Proton Solvation and Transport in Aqueous and

Biomolecular Systems. *Acc. Chem. Res.* **2006**, *39*, 143–150.

- (31) Frängsmyr, T. *Communiqué de Presse: Le Prix Nobel de Chimie de 1999*; Almqvist & Wiksell: Stockholm, 2000.
- (32) Terenin, A.; Kariakin, A. Proton Transfer between Organic Molecules Caused by Light. *Nature* **1947**, *159*, 881–882.
- (33) Kasha, M. Proton-Transfer Spectroscopy. Perturbation of the Tautomerization Potential. *J. Chem. Soc. Faraday Trans. 2* **1986**, *82*, 2379.
- (34) Arnaut, L. G.; Formosinho, S. J. Excited-State Proton Transfer Reactions I. Fundamentals and Intermolecular Reactions. *J. Photochem. Photobiol. A Chem.* **1993**, *75*, 1–20.
- (35) Formosinho, S. J.; Arnaut, L. G. Excited-State Proton Transfer Reactions II. Intramolecular Reactions. *J. Photochem. Photobiol. A Chem.* **1993**, *75*, 21–48.
- (36) Agmon, N. Elementary Steps in Excited-State Proton Transfer. *J. Phys. Chem. A* **2005**, *109*, 13–35.
- (37) Tolbert, L. M.; Solntsev, K. M. Excited-State Proton Transfer: From Constrained Systems to “Super” Photoacids to Superfast Proton Transfer. *Acc. Chem. Res.* **2002**, *35*, 19–27.
- (38) Demchenko, A. P.; Tang, K.-C.; Chou, P.-T. Excited-State Proton Coupled Charge Transfer Modulated by Molecular Structure and Media Polarization. *Chem. Soc. Rev.* **2013**, *42*, 1379–1408.
- (39) Douhal, A.; Lahmani, F.; Zewail, A. H. Proton-Transfer Reaction Dynamics. *Chem. Phys.* **1996**, *207*, 477–498.
- (40) Kuzmin, M. G.; Soboleva, I. V.; Ivanov, V. L.; Gould, E.-A.; Huppert, D.; Solntsev, K. M.

Competition and Interplay of Various Intermolecular Interactions in Ultrafast Excited-State Proton and Electron Transfer Reactions. *J. Phys. Chem. B* **2014**.

- (41) Kijak, M.; Nosenko, Y.; Singh, A.; Thummel, R. P.; Waluk, J. Mode-Selective Excited-State Proton Transfer in 2-(2'-Pyridyl)pyrrole Isolated in a Supersonic Jet. *J. Am. Chem. Soc.* **2007**, *129*, 2738–2739.
- (42) Kwon, O. H.; Lee, Y. S.; Park, H. J.; Kim, Y.; Jang, D. J. Asymmetric Double Proton Transfer of Excited 1:1 7-Azaindole/Alcohol Complexes with Anomalously Large and Temperature-Independent Kinetic Isotope Effects. *Angew. Chem. Int. Ed.* **2004**, *43*, 5792–5796.
- (43) Kwon, O.-H.; Mohammed, O. F. Water-Wire Catalysis in Photoinduced Acid-Base Reactions. *Phys. Chem. Chem. Phys.* **2012**, *14*, 8974–8980.
- (44) Mohammed, O. F. Sequential Proton Transfer Through Water Bridges in Acid-Base Reactions. *Science*, **2005**, *310*, 83–86.
- (45) Kim, T. G.; Topp, M. R. Ultrafast Excited-State Deprotonation and Electron Transfer in Hydroxyquinoline Derivatives. *J. Phys. Chem. A* **2004**, *108*, 10060–10065.
- (46) Benesi, H. a.; Hildebrand, J. H. The Benesi-Hildebrand Method for Determination of K_f for DA Association and ϵ Values for DA CT Absorption. *J. Am. Chem. Soc.* **1949**, *71*, 2703.
- (47) Park, S.-Y.; Kim, B.; Lee, Y.-S.; Kwon, O.-H.; Jang, D.-J. Triple Proton Transfer of Excited 7-Hydroxyquinoline along a Hydrogen-Bonded Water Chain in Ethers: Secondary Solvent Effect on the Reaction Rate. *Photochem. Photobiol. Sci.* **2009**, *8*, 1611.
- (48) Pérez-Lustres, J. L.; Rodríguez-Prieto, F.; Mosquera, M.; Senyushkina, T. a; Ernsting, N. P.; Kovalenko, S. a. Ultrafast Proton Transfer to Solvent: Molecularity and Intermediates from Solvation- and Diffusion-Controlled Regimes. *J. Am. Chem. Soc.* **2007**, *129*, 5408–5418.

- (49) Solntsev, K. M.; Huppert, D.; Agmon, N. Photochemistry of “Super”-Photoacids. Solvent Effects. *J. Phys. Chem. A* **1999**, *103*, 6984–6997.
- (50) Poole, S. K.; Poole, C. F. Characterization of Surfactant Selectivity in Micellar Electrokinetic Chromatography. *Analyst* **1997**, *122*, 267–274.
- (51) Park, S.-Y.; Lee, Y. M.; Kwac, K.; Jung Y.; Kwon, O.-H. Alcohol Dimer is Requisite to Form an Alkyl Oxonium Ion in the Proton Transfer of a Strong (Photo)acid to Alcohol. *Submitted*.

Acknowledgements

Without many people's help, I could not complete this thesis. I appreciate all the members in the Prof. Oh-Hoon Kwon's lab.

First of all, I appreciate advisor, Prof. Oh-Hoon Kwon, for giving me great opportunity to do master's degree in UNIST. Also, He told me many scientific knowledge and aspects. With his encouragement and support in the research, I could finish this project and I could write this thesis.

I also thanks Young Min Lee for synthesizing *N*-methyl-7-hydroxyquinolium and great help for preparing this thesis. And thanks Dr. Sun-Young Park for kind explanation and encouragement with my data analysis.